Published OnlineFirst October 13, 2010; DOI: 10.1158/1078-0432.CCR-10-0387

not considered DLT. Although 9 of 15 patients at a dose level of 20 to 28 mg/m^2 had either a delay or a reduction in treatment as a result of toxicity (especially neutropenia), only 3 of these patients required dose reduction after DLT; even in the 28 mg/m^2 cohort, 6 of 8 patients successfully continued treatment with NK012 without dose reduction.

Toxicity

NK012 was generally well tolerated. All patients reported AEs considered to be related to NK012, most of which were asymptomatic and grade 1 to 2 in severity: nausea, anorexia, vomiting, fatigue, elevated AST/ALT, elevated γ-glutamyl transpeptidase (γ-GTP), and thrombocytopenia. Three infusion-related reactions were observed at a dose level of 2, 12, and 24 mg/m^2. No cholinergic reactions were observed; such reactions sometimes occur during CPT-11 administration. Fifteen patients reported 36 grade 3 to 4 drug-related AEs (Table 3). The most common grade 3 to 4 events were leukopenia and neutropenia. The median time to the neutrophil nadir at a dose level of 28 mg/m^2 was 12 days (range, 9-21 days), with recovery to grade 1 within 4 to 16 days in cycle 1. No grade 3 or 4 diarrhea was observed.

Four patients reported five serious AEs, three of which were deemed possibly related to NK012: grade 3 infection with neutropenia, grade 4 neutropenia, and grade 3 atrial flutter.

Two of the nine patients treated at a dose level of 28 mg/m^2 experienced DLT during cycle 1. In another independent phase I study of NK012 in the United States, only one of six patients experienced DLT at 28 mg/m^2 during cycle 1, but two of five patients experienced DLT at 37 mg/m^2 during cycle 1 (22). Although the protocol definition of MTD had not been reached, the Efficacy and Safety Assessment Committee recommended discontinuing dose escalation according to the hematologic toxicity profile of our study and another independent phase I study (22). The recommended phase II dose was determined to be 28 mg/m^2 with at least a 3-week interval between treatment cycles.

Table 2. Dose-escalation schema and DLT

NK012 dose (mg/m^2)	Total	DLT			
		Cycle 1	Cycle 2	Cycle 3	Cycle 4
2	1	0	0	0	0
4	1	0	0	0	0
8	1	0	0	0	0
12	3	0	0	0	0
16	3	0	0	0	1*
20	3	0	0	0	0
24	3	0	0	1†	0
28‡	9	2†	1†	1†	1§

*γ-GTP increased.
†Neutropenia or a related event.
‡Recommended dose for phase II studies.
§Atrial flutter.

Efficacy

Twenty-three patients were assessable for response. Two patients had confirmed partial response at a dose of 28 mg/m^2. The first patient, who received CDDP + 5-fluorouracil combination chemotherapy followed by docetaxel monotherapy and had a previously progressing esophageal cancer, achieved a partial response confirmed by CT and continued this therapy for 5 months (serial CT scans can be seen in Supplementary Data). The second patient had a recurrence of lung carcinoid tumor. He developed multiple liver and bone metastases and enrolled in this phase I study because there is no standard systemic chemotherapy for his disease. After four cycles, a partial response was documented. He continued to receive this chemotherapy for 12 months until disease progression. Nine patients had stable disease. In 12 colorectal cancer patients, who were refractory to CPT-11 and oxaliplatin, 5 patients had stable diseases, 4 of whom successfully received six cycles of treatment or more.

Pharmacokinetics

The mean plasma concentration-time profile of polymer-bound SN-38, SN-38, and SN-38G at a dose of 28 mg/m^2 (recommended phase II dose) is shown in Fig. 2A. The concentrations of these analytes in the plasma were maintained over an extended period of time, indicating that NK012 achieved prolonged exposure. There was a proportional increase in C_{max} and $AUC_{inf.}$ values with dose (Fig. 2B and C). The PK parameters are summarized in Table 4. The $t_{1/2z}$ of bound SN-38 was 36.0 to 168 hours, CL_{tot} was 98.8 to 150 mL/h/m^2, V_{ss} was 2,020 to 4,050 mL/m^2, and $MRT_{inf.}$ was 15.9 to 28.6 hours. No significant differences in these parameters were seen in the dose range from 2 to 28 mg/m^2. The $t_{1/2z}$ of SN-38 ranged from 70.7 to 266 hours, and $MRT_{inf.}$ ranged from 47.3 to 109 hours. These parameters were dose independent. Therefore, PK of NK012 proved to be linear in the dose range of 2 to 28 mg/m^2. There was no obvious difference between the plasma concentration of the respective analytes in cycles 1 and 2 (data not shown), although the study design could not fully evaluate the cycle dependency of NK012 PK. The cumulative urinary excretion rate (0-48 hours) of total SN-38 and SN-38G at a dose level of 28 mg/m^2 was 7.0% and 6.8%, respectively. These rates were independent of the dose escalation.

Discussion

In this phase I study, NK012 was well tolerated at doses <28 mg/m^2 every 3 weeks.

Observed toxicity was consistent with CPT-11, a prodrug of SN-38. DLT associated with NK012 was mainly neutropenia. Therefore, it is necessary to pay attention to neutrophil count changes after treatment with NK012; patients with a decreased count should be carefully monitored to prevent infection. Infusion-related reactions characterized by flushing, chest discomfort, or itching occur sometimes during the administration of liposomal

Published OnlineFirst October 13, 2010; DOI: 10.1158/1078-0432.CCR-10-0387

Table 3. Highest hematologic and nonhematologic toxicity per patient

A. Hematologic toxicity

Dose (mg/m^2)	*n*	Leukopenia				Neutropenia				Thrombocytopenia			
		Grade				Grade				Grade			
		1	2	3	4	1	2	3	4	1	2	3	4
2	1	0	0	0	0	0	0	0	0	0	0	0	0
4	1	0	0	0	0	0	0	0	0	0	0	0	0
8	1	0	0	0	0	0	0	0	0	0	0	0	0
12	3	0	1	1	0	1	0	1	0	1	0	1	0
16	3	1	2	0	0	2	0	1	0	1	0	0	0
20	3	1	0	2	0	1	0	0	2	0	1	0	0
24	3	0	2	1	0	0	0	2	1	3	0	0	0
28	9	0	1	5	3	0	0	4	5	3	3	0	0
Total	24	2	6	9	3	4	0	8	8	8	4	1	0

B. Nonhematologic toxicity

	2-20 mg/m^2 (*n* = 12)				24 mg/m^2 (*n* = 3)				28 mg/m^2 (*n* = 9)			
	Grade				Grade				Grade			
	1	2	3	4	1	2	3	4	1	2	3	4
Nausea	8	2	0	0	3	0	0	0	3	3	1	0
Anorexia	6	3	0	0	3	0	0	0	3	2	2	0
Diarrhea	3	0	0	0	0	1	0	0	4	4	0	0
Vomiting	3	1	0	0	0	0	0	0	2	3	0	0
Fatigue	7	0	0	0	2	1	0	0	4	2	0	0
Febrile neutropenia	0	0	0	0	0	0	0	0	0	0	1	0
Infection	0	1	0	0	0	0	0	0	0	0	1	0
Atrial flutter	0	0	0	0	0	0	0	0	0	0	1	0
Alopecia	7	1	—	—	1	2	—	—	5	3	—	—
γ-GTP	0	1	1	0	1	0	0	0	2	1	0	0
Rash	2	1	0	0	1	1	0	0	1	2	0	0

and antibody drugs. In this study, only three infusion-related reactions were observed at dose levels of 2, 12, and 24 mg/m^2. However, these infusion reactions were grade 1 and deemed non–dose dependent. The factors associated with the infusion-related reactions remain to be explained. Diarrhea, which is known as a DLT of CPT-11, was mild and transient in this study. Fatigue, nausea, and anorexia were also commonly experienced AEs but were mild and transient. Our preclinical study showed that the CPT-11–induced intestinal mucosal change in mice was active inflammation with cellular invasion, deformed glandular alignment, and glandular duct disappearance. On the other hand, the intestinal mucosa in mice in the NK012 treatment group was almost the same as that in the saline treatment group (14). CPT-11, SN-38, and SN-38G are excreted into the bile and eventually reach the small intestinal lumen (23, 24). SN-38G is deconjugated in the cecum and colon to regenerate SN-38 through bacterial β-glucuronidase (25). Because the CPT-11 dose in the preclinical study was 3-fold higher than that of NK012 at the SN-38 equivalent dose, a higher amount of CPT-11 was found in the intestinal lumen. It is speculated that the highly excreted CPT-11 was reabsorbed in the small intestinal epithelium and converted to SN-38, causing damage to the intestinal mucosa (14). It is too early to conclude that NK012 may cause weaker diarrhea than CPT-11, but the present results within a phase I setting may encourage further clinical evaluation about intestinal toxicity of NK012.

The PK analysis of NK012 suggested that the tissue distribution of SN-38–incorporating micelles is limited. This is consistent with the data obtained in our preclinical study (13). In a phase I study of CPT-11 at doses of 100 to 750 mg/m^2, it was reported that the CL_{tot} and V_{ss} of CPT-11 were 15,000 mL/h/m^2 and 157,000 mL/m^2, respectively (26). Therefore, the present study revealed that the CL_{tot} and V_{ss} of polymer-bound SN-38 were, respectively, approximately 150- and 80-fold lower than those of CPT-11. This suggests that NK012 may have a low distribution in normal tissue after administration. On the other hand, in tumor tissue, we speculate that NK012 accumulates to a greater extent and stays longer in tumor tissue due to the enhanced permeability and retention effect

Published OnlineFirst October 13, 2010; DOI: 10.1158/1078-0432.CCR-10-0387

(27) because it is stable in circulation and exhibits a markedly higher plasma AUC than CPT-11. Moreover, NK012 seems to induce sustained release of SN-38 inside the tumor following the accumulation of NK012 in the tumor tissue (13–18).

Sustained exposure to SN-38 is required for successful CPT-11–based chemotherapy because SN-38 induced single-strand DNA breaks in the presence of topoisomerase I and is only effective during the relatively short S phase of the cell cycle (28). When compared with SN-38 converted from conventional CPT-11 at a dose of 250 mg/m^2 (29), SN-38 released from NK012 at 28 mg/m^2 exhibited 2.4-fold greater systemic exposure (0.876 versus 2.12 μg·h/mL) and 15-fold slower elimination from plasma (13.9 versus 209 hours). This result was compatible

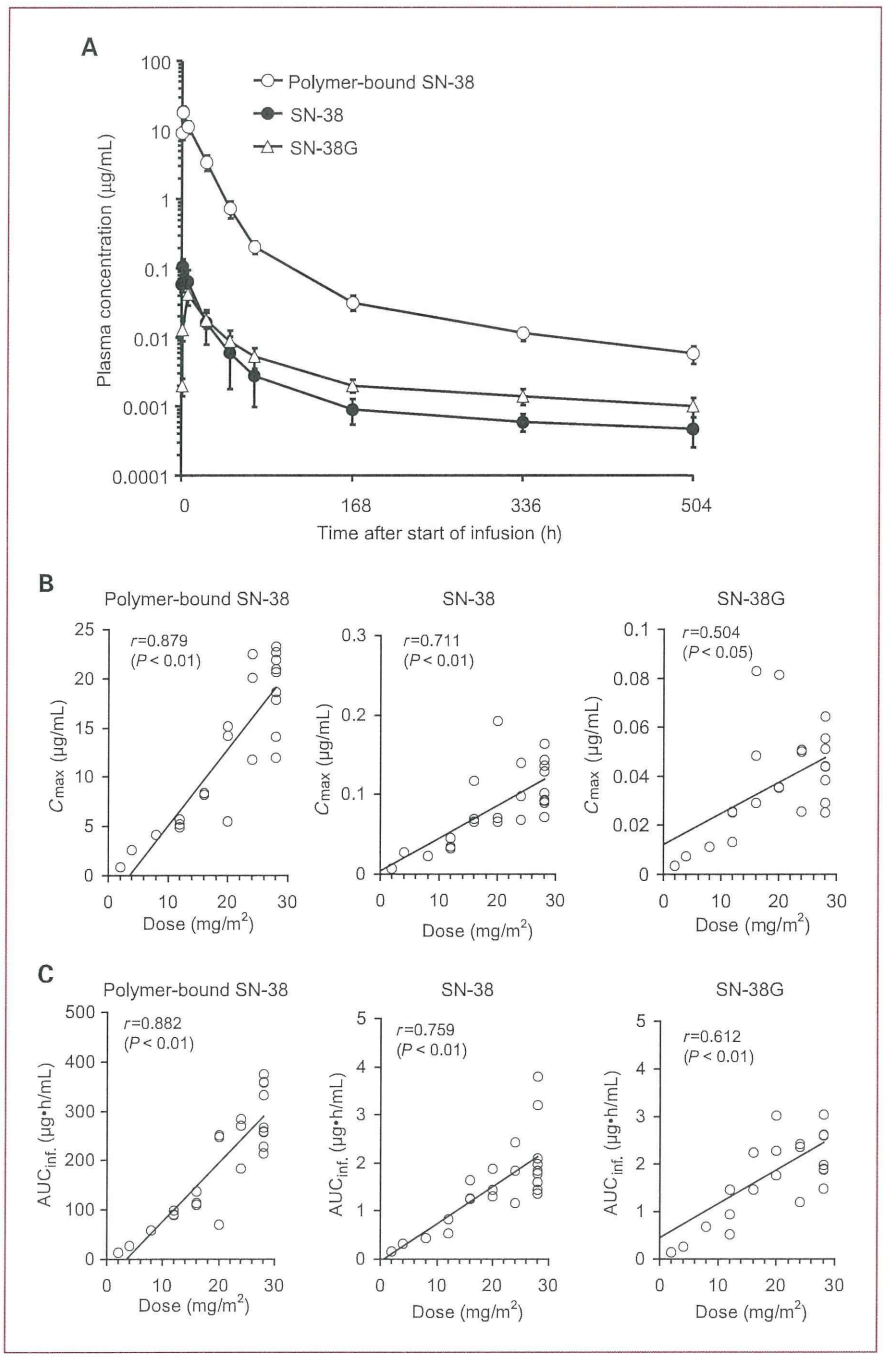

Fig. 2. A, plasma concentration-time profile of polymer-bound SN-38, SN-38, and SN-38G in nine patients after an infusion of NK012 at 28 mg/m^2 in cycle 1. Points, mean; bars, SD. Relationship between dose and C_{max} (B) and between dose and $AUC_{inf.}$ (C) of respective analytes in 23 or 24 patients after an infusion of NK012 in cycle 1.

Published OnlineFirst October 13, 2010; DOI: 10.1158/1078-0432.CCR-10-0387

Table 4. Plasma PK parameters of (A) polymer-bound SN-38, (B) SN-38, and (C) SN-38G in cycle 1

Dose (mg/m^2)	No. patients	Mean (SD)						
		C_{max} (μg/mL)	T_{max} (h)	$t_{1/2z}$ (h)	$AUC_{inf.}$ (μg·h/mL)	$MRT_{inf.}$ (h)	CL_{tot} ($mL/h/m^2$)	V_{ss} (mL/m^2)
A. Polymer-bound SN-38								
2	1	0.91	1	128	14.1	28.6	142	4,050
4	1	2.60	0.6	36.0	27.0	15.9	148	2,370
8	1	4.16	0.5	102	57.8	19.1	138	2,640
12	3	5.32 (0.38)	0.7 (0.3)	135 (8)	92.4 (5.5)	25.3 (4.0)	130 (7)	3,270 (330)
16	3	8.32 (0.11)	0.8 (0.3)	168 (41)	120 (15)	28.2 (4.0)	134 (15)	3,830 (940)
20	3	11.6 (5.3)	0.8 (0.3)	128 (28)	189 (104)	24.3 (2.0)	150 (121)	3,730 (3,190)
24	3	18.1 (5.6)	0.7 (0.3)	128 (13)	246 (55)	24.5 (0.9)	101 (26)	2,480 (600)
28	9	19.1 (3.9)	0.7 (0.3)	137 (19)	294 (62)	22.2 (2.3)	98.8 (20.6)	2,020 (530)
B. SN-38								
2	1	0.01	1	70.7	0.16	47.3	N/A	N/A
4	1	0.03	0.6	179	0.32	99.9	N/A	N/A
8	1	0.02	1	107	0.430	54.5	N/A	N/A
12	3	0.0377 (0.0073)	0.8 (0.3)	193*	0.683*	70.6*	N/A	N/A
16	3	0.0841 (0.0285)	0.8 (0.3)	250 (60)	1.38 (0.23)	91.4 (23.7)	N/A	N/A
20	3	0.110 (0.072)	0.7 (0.3)	266 (40)	1.55 (0.30)	104 (19)	N/A	N/A
24	3	0.102 (0.036)	0.7 (0.3)	216 (24)	1.81 (0.64)	109 (20)	N/A	N/A
28	9	0.114 (0.031)	0.8 (0.3)	209 (25)	2.12 (0.83)	95.7 (16.7)	N/A	N/A
C. SN-38G								
2	1	0	6	42.7	0.15	50.9	N/A	N/A
4	1	0.01	6	30.8	0.27	38.3	N/A	N/A
8	1	0.01	6	72.9	0.68	75.1	N/A	N/A
12	3	0.02 (0.0071)	6 (0)	171 (102)	0.97 (0.471)	148 (92)	N/A	N/A
16	3	0.05 (0.0272)	6 (0)	294 (61)	2.62 (1.39)	221 (80)	N/A	N/A
20	3	0.05 (0.0266)	6 (0)	264 (70)	2.36 (0.63)	212 (49)	N/A	N/A
24	3	0.0420 (0.0143)	6 (0)	222 (18)	2.00 (0.68)	193 (11)	N/A	N/A
28	9	0.04 (0.0132)	6 (0)	205 (20)	2.28 (0.57)	186 (27)	N/A	N/A

NOTE: Values are represented as the mean (SD).

Abbreviation: N/A, not available.

*n = 2. One patient at 12 mg/m^2 was excluded from the analysis due to the presence of an interference peak on the HPLC chromatogram.

with those obtained in preclinical studies (13, 14, 17). Therefore, the longer systemic exposure time of SN-38 achieved with NK012 therapy is also expected to improve therapeutic efficacy.

Overall, our data suggest that polymer-bound SN-38 and released SN-38 exhibit a linear PK in the dose range of 2 to 28 mg/m^2. In several phase I studies of CPT-11, it was reported that the C_{max} and/or the AUC of CPT-11 increased linearly with the dosage, but the AUC of SN-38 was not as dose dependent as that of CPT-11 or it has no correlation with the dose due to considerable interpatient variability (29–32). Several metabolizing enzymes (e.g., CEs, UGT1A, and CYP3A4) are involved in the disposition of CPT-11 (8, 9, 33). NK012, unlike CPT-11, is hydrolyzed nonenzymatically to release SN-38, resulting in a dose-proportional increase in systemic exposure. Thus, NK012 proved to function steadily as a drug carrier in a dose-independent manner and to release SN-38 in a dose-dependent manner in this phase I trial. In the independent phase I trial conducted in the United States, the PK profile and toxic profile including diarrhea were similar to those of our study. The DLT of the U.S. study was neutropenia and pneumonia with neutropenia. The MTD in the U.S. trial was also determined to be 28 mg/m^2 (22).

In conclusion, the recommended phase II dose of NK012 is 28 mg/m^2 with at least a 3-week interval between treatment cycles. The favorable safety profile and promising clinical antitumor activity warrant further clinical evaluation.

Published OnlineFirst October 13, 2010; DOI: 10.1158/1078-0432.CCR-10-0387

Disclosure of Potential Conflicts of Interest

T. Hamaguchi: research grant, Nippon Kayaku Co. Ltd.

Acknowledgments

We thank the patients who participated in this trial, Dr. Toshiharu Yamaguchi for serving as medical consultant, and Kaoru Shiina and Hiromi Orita for their secretarial assistance.

Grant Support

Nippon Kayaku Co. Ltd.
The costs of publication of this article were defrayed in part by the payment of page charges. This article must therefore be hereby marked *advertisement* in accordance with 18 U.S.C. Section 1734 solely to indicate this fact.

Received 02/15/2010; revised 08/05/2010; accepted 08/25/2010; published OnlineFirst 10/12/2010.

References

1. Bodurka DC, Levenback C, Wolf JK, et al. Phase II trial of irinotecan in patients with metastatic epithelial ovarian cancer or peritoneal cancer. J Clin Oncol 2003;21:291–7.
2. Douillard JY, Cunningham D, Roth AD, et al. Irinotecan combined with fluorouracil compared with fluorouracil alone as first-line treatment for metastatic colorectal cancer: a multicentre randomised trial. Lancet 2000;355:1041–7.
3. Negoro S, Masuda N, Takada Y, et al. Randomised phase III trial of irinotecan combined with cisplatin for advanced non-small-cell lung cancer. Br J Cancer 2003;88:335–41.
4. Noda K, Nishiwaki Y, Kawahara M, et al. Irinotecan plus cisplatin compared with etoposide plus cisplatin for extensive small-cell lung cancer. N Engl J Med 2002;346:85–91.
5. Saltz LB, Cox JV, Blanke C, et al, Irinotecan Study Group. Irinotecan plus fluorouracil and leucovorin for metastatic colorectal cancer. N Engl J Med 2000;343:905–14.
6. Takimoto CH, Arbuck S. Topoisomerase I targeting agents: the camptothecines. In: Chabner BA, Lango DL, editors. Cancer Chemotherapy and Biotherapy: Principles and Practice. 3rd edition, Philadelphia: Lippincott Willams & Wilkins; 2001. p. 579–646.
7. Rothenberg ML, Kuhn JG, Burris HA III, et al. Phase I and pharmacokinetic trial of weekly CPT-11. J Clin Oncol 1993;11:2194–204.
8. Slatter JG, Schaaf LJ, Sams JP, et al. Pharmacokinetics, metabolism, and excretion of irinotecan (CPT-11) following I.V. infusion of [(14)C] CPT-11 in cancer patients. Drug Metab Dispos 2000;28:423–33.
9. Guichard S, Terret C, Hennebelle I, et al. CPT-11 converting carboxylesterase and topoisomerase activities in tumour and normal colon and liver tissues. Br J Cancer 1999;80:364–70.
10. Matsumura Y, Kataoka K. Preclinical and clinical studies of anticancer agent-incorporating polymer micelles. Cancer Sci 2009;100:572–9.
11. Gordon AN, Fleagle JT, Guthrie D, Parkin DE, Gore ME, Lacave AJ. Recurrent epithelial ovarian carcinoma: a randomized phase III study of pegylated liposomal doxorubicin versus topotecan. J Clin Oncol 2001;19:3312–22.
12. Gradishar WJ, Tjulandin S, Davidson N, et al. Phase III trial of nanoparticle albumin-bound paclitaxel compared with polyethylated castor oil-based paclitaxel in women with breast cancer. J Clin Oncol 2005;23:7794–803.
13. Koizumi F, Kitagawa M, Negishi T, et al. Novel SN-38-incorporating polymeric micelles, NK012, eradicate vascular endothelial growth factor-secreting bulky tumors. Cancer Res 2006;66:10048–56.
14. Nagano T, Yasunaga M, Goto K, et al. Antitumor activity of NK012 combined with cisplatin against small cell lung cancer and intestinal mucosal changes in tumor-bearing mouse after treatment. Clin Cancer Res 2009;15:4348–55.
15. Saito Y, Yasunaga M, Kuroda J, Koga Y, Matsumura Y. Enhanced distribution of NK012, a polymeric micelle-encapsulated SN-38, and sustained release of SN-38 within tumors can beat a hypovascular tumor. Cancer Sci 2008;99:1258–64.
16. Sumitomo M, Koizumi F, Asano T, et al. Novel SN-38-incorporated polymeric micelle, NK012, strongly suppresses renal cancer progression. Cancer Res 2008;68:1631–5.
17. Kuroda J, Kuratsu J, Yasunaga M, Koga Y, Saito Y, Matsumura Y. Potent antitumor effect of SN-38-incorporating polymeric micelle, NK012, against malignant glioma. Int J Cancer 2009;124:2505–11.
18. Nakajima TE, Yanagihara K, Takigahira M, et al. Antitumor effect of SN-38-releasing polymeric micelles, NK012, on spontaneous peritoneal metastases from orthotopic gastric cancer in mice compared with irinotecan. Cancer Res 2008;68:9318–22.
19. Nakajima TE, Yasunaga M, Kano Y, et al. Synergistic antitumor activity of the novel SN-38-incorporating polymeric micelles, NK012, combined with 5-fluorouracil in a mouse model of colorectal cancer, as compared with that of irinotecan plus 5-fluorouracil. Int J Cancer 2008;122:2148–53.
20. Simon R, Freidlin B, Rubinstein L, Arbuck SG, Collins J, Christian MC. Accelerated titration designs for phase I clinical trials in oncology. J Natl Cancer Inst 1997;89:1138–47.
21. Matsumura Y, Hamaguchi T, Ura T, et al. Phase I clinical trial and pharmacokinetic evaluation of NK911, a micelle-encapsulated doxorubicin. Br J Cancer 2004;91:1775–81.
22. HA Burris I, Infante JR, Spigel DR, et al. A phase I dose-escalation study of NK012 [abstract 2538]. J Clin Oncol 2008;26.
23. Atsumi R, Suzuki W, Hakusui H. Identification of the metabolites of irinotecan, a new derivative of camptothecin, in rat bile and its biliary excretion. Xenobiotica 1991;21:1159–69.
24. Chu XY, Kato Y, Sugiyama Y. Multiplicity of biliary excretion mechanisms for irinotecan, CPT-11, and its metabolites in rats. Cancer Res 1997;57:1934–8.
25. Takasuna K, Hagiwara T, Hirohashi M, et al. Involvement of β-glucuronidase in intestinal microflora in the intestinal toxicity of the antitumor camptothecin derivative irinotecan hydrochloride (CPT-11) in rats. Cancer Res 1996;56:3752–7.
26. Abigerges D, Chabot G, Armand J, Herait P, Gouyette A, Gandia D. Phase I and pharmacologic studies of the camptothecin analog irinotecan administered every 3 weeks in cancer patients. J Clin Oncol 1995;13:210–21.
27. Matsumura Y, Maeda H. A new concept for macromolecular therapeutics in cancer chemotherapy: mechanism of tumoritropic accumulation of proteins and the antitumor agent smancs. Cancer Res 1986;46:6387–92.
28. Gerrits CJ, de Jonge MJ, Schellens JH, Stoter G, Verweij J. Topoisomerase I inhibitors: the relevance of prolonged exposure for present clinical development. Br J Cancer 1997;76:952–62.
29. Taguchi T, Wakui A, Hasegawa K, et al. Phase I clinical study of CPT-11. Research group of CPT-11. Gan To Kagaku Ryoho 1990;17:115–20.
30. de Forni M, Bugat R, Chabot GG, et al. Phase I and pharmacokinetic study of the camptothecin derivative irinotecan, administered on a weekly schedule in cancer patients. Cancer Res 1994;54:4347–54.
31. Pitot HC, Goldberg RM, Reid JM, et al. Phase I dose-finding and pharmacokinetic trial of irinotecan hydrochloride (CPT-11) using a once-every-three-week dosing schedule for patients with advanced solid tumor malignancy. Clin Cancer Res 2000;6:2236–44.
32. Rothenberg ML, Kuhn JG, Schaaf LJ, et al. Phase I dose-finding and pharmacokinetic trial of irinotecan (CPT-11) administered every two weeks. Ann Oncol 2001;12:1631–41.
33. Haaz MC, Rivory L, Riche C, Vernillet L, Robert J. Metabolism of irinotecan (CPT-11) by human hepatic microsomes: participation of cytochrome P-450 3A and drug interactions. Cancer Res 1998;58:468–72.

Drug Metab. Pharmacokinet. 25 (6): 578–587 (2010).

Regular Article

Genetic Polymorphisms of *FCGRT* Encoding FcRn in a Japanese Population and Their Functional Analysis

Akiko ISHII-WATABE[1,a], Yoshiro SAITO[2,3,b,*], Takuo SUZUKI[1], Minoru TADA[1], Maho UKAJI[2], Keiko MAEKAWA[2,3], Kouichi KUROSE[2,3], Nahoko KANIWA[2,3], Jun-ichi SAWADA[2,4,**], Nana KAWASAKI[1], Teruhide YAMAGUCHI[1], Takako EGUCHI NAKAJIMA[5,†], Ken KATO[5], Yasuhide YAMADA[5], Yasuhiro SHIMADA[5], Teruhiko YOSHIDA[6], Takashi URA[7], Miyuki SAITO[7], Kei MURO[7], Toshihiko DOI[8], Nozomu FUSE[8], Takayuki YOSHINO[8], Atsushi OHTSU[8,9], Nagahiro SAIJO[10,††], Tetsuya HAMAGUCHI[5], Haruhiro OKUDA[2,4] and Yasuhiro MATSUMURA[11]

[1]*Division of Biological Chemistry and Biologicals, National Institute of Health Sciences, Tokyo, Japan*
[2]*Project Team for Pharmacogenetics, National Institute of Health Sciences, Tokyo, Japan*
[3]*Division of Medicinal Safety Sciences, National Institute of Health Sciences, Tokyo, Japan*
[4]*Division of Organic Chemistry, National Institute of Health Sciences, Tokyo, Japan*
[5]*Gastrointestinal Oncology Division, National Cancer Center Hospital, Tokyo, Japan*
[6]*Genetics Division, National Cancer Center Research Institute, National Cancer Center, Tokyo, Japan*
[7]*Department of Medical Oncology, Aichi Cancer Center Hospital, Nagoya, Japan*
[8]*Division of Gastrointestinal Oncology/Digestive Endoscopy, National Cancer Center Hospital East, Kashiwa, Japan*
[9]*Director of Research Center for Innovative Oncology, National Cancer Center Hospital East, Kashiwa, Japan*
[10]*Deputy Director, National Cancer Center Hospital East, Kashiwa, Japan*
[11]*Investigative Treatment Division, National Cancer Center Hospital East, Kashiwa, Japan*
[a,b]*Akiko Ishii-Watabe and Yoshiro Saito contributed equally to this work*

Full text of this paper is available at http://www.jstage.jst.go.jp/browse/dmpk

Summary: Neonatal Fc receptor (FcRn) plays an important role in regulating IgG homeostasis in the body. Changes in FcRn expression levels or activity caused by genetic polymorphisms of *FCGRT*, which encodes FcRn, may lead to interindividual differences in pharmacokinetics of therapeutic antibodies. In this study, we sequenced the 5′-flanking region, all exons and their flanking regions of *FCGRT* from 126 Japanese subjects. Thirty-three genetic variations, including 17 novel ones, were found. Of these, two novel non-synonymous variations, 629G>A (R210Q) and 889T>A (S297T), were found as heterozygous variations. We next assessed the functional significance of the two novel non-synonymous variations by expressing wild-type and variant proteins in HeLa cells. Both variant proteins showed similar intracellular localization as well as antibody recycling efficiencies. These results suggested that at least no common functional polymorphic site with amino acid change was present in the *FCGRT* of our Japanese population.

Keywords: ***FCGRT*; neonatal Fc receptor (FcRn); genetic polymorphism; novel non-synonymous variation**

Received; July 19, 2010, Accepted; September 14, 2010, J-STAGE Advance Published Date; October 1, 2010
**To whom correspondence should be addressed:* Yoshiro SAITO, PhD, *Division of Medicinal Safety Sciences, National Institute of Health Sciences, 1-18-1 Kamiyoga, Setagaya-ku, Tokyo 158-8501, Japan. Tel. +81-3-3700-9528, Fax. +81-3-3700-9788, E-mail: yoshiro@nihs.go.jp*
***Present address: Pharmaceuticals and Medical Devices Agency, Shin-Kasumigaseki Building, 3-3-2 Kasumigaseki, Chiyoda-ku, Tokyo 100-0013, Japan.*
†Present address: Department of Clinical Oncology, St. Marianna University School of Medicine, 2-16-1 Sugao, Miyamae-ku, Kawasaki-city 216-8511, Japan.
††Present address: Kinki University School of Medicine, 377-2 Ohno-Higashi, Osaka-Sayama City, Osaka 589-8511, Japan.
This study was supported in part by the Program for the Promotion of Fundamental Studies in Health Sciences from the National Institute of Biomedical Innovation, and by the Health and Labor Sciences Research Grants from the Ministry of Health, Labor and Welfare of Japan, and by KAKENHI (20590167) from the Japan Society for the Promotion of Science (JSPS).

Introduction

Neonatal Fc receptor (FcRn) is an immunoglobulin G (IgG) receptor related to major histocompatibility (MHC) class I molecules.[1,2] Like MHC class I, FcRn consists of a heavy chain with extracellular α1, α2, and α3 domains followed by a transmembrane segment and a short cytoplasmic tail and non-covalently bound β2-microglobulin (β2m). FcRn binds the Fc region of monomeric IgG. The FcRn heavy chain is encoded by *FCGRT*, which is located in chromosome 19q13.3 and comprises 6 exons.

In humans, FcRn expression has been observed in a wide variety of tissues including placenta, liver, kidney and vascular endothelium.[1] FcRn has multiple roles in the body such as absorption or secretion of IgG across the intestinal mucosa, and IgG recycling from endothelial cells. With regard to antibody recycling, FcRn binds to the Fc domain of IgG at acidic pH in endosomes after endocytosis, and recycles it back to the extracellular space via the exocytic pathway, thereby protecting IgG from intracellular degradation in lysosomes.[2] This mechanism contributes to the long serum half-life of IgG, and thus, IgG recycling activity is an important function of FcRn and could contribute to the efficacy of antibody therapeutics. Indeed, we previously reported that affinities of antibody therapeutics to FcRn were closely correlated with the serum half-lives reported in clinical studies.[3] The relatively short serum half-life of Fc-fusion proteins such as etanercept, a fusion protein consisting of the extracellular ligand-binding portion of the human tumor necrosis factor receptor linked to the Fc portion of human IgG1, is thought to arise from low affinity to FcRn.[3]

Genetic polymorphisms of genes related to drug metabolism and transport are one of the crucial factors for low-molecular-weight drugs. Pharmacokinetics or pharmacodynamics of biologicals including antibody therapeutics may also be influenced by genetic polymorphisms of transport or target proteins. In this context, changes in FcRn expression levels or activity caused by genetic polymorphisms of *FCGRT* may lead to interindividual differences in pharmacokinetics of antibody therapeutics. However, reports on *FCGRT* genetic polymorphisms in Japanese populations are lacking.

Here we sequenced the 5′-flanking region, all exons and their flanking regions of *FCGRT* from 126 Japanese subjects. We then examined the functional properties of two detected non-synonymous variations using mammalian expression systems focusing on intracellular localization and antibody recycling activities.

Materials and Methods

Human genomic DNA samples: One hundred twenty-six Japanese cancer patients participated in this study. The ethical review boards of the National Cancer Center, Aichi Cancer Center and the National Institute of Health Sciences approved this study. Written informed consent was obtained from all subjects. Genomic DNA for DNA sequencing was extracted from blood leukocytes.

PCR conditions for DNA sequencing: The following sequences obtained from GenBank were used for primer design and reference sequences: NW_927240.1 (genome) and NM_004107.3 (mRNA). For sequencing, two sets of long-range PCR were performed to amplify all 6 exons from 50 ng of genomic DNA with two sets of primers (0.5 μM) designed in the promoter or intronic regions as listed in "1st PCR" of **Table 1**. We used LA-Taq with GC buffer I (0.05 U/μl, Takara Bio Inc., Shiga, Japan) to amplify from the 5′-flanking region to exon 3 and Z-Taq (0.025 U/μl, Takara Bio. Inc.) from exons 4 to 6, as described in **Table 1**. The 1st PCR conditions were 94°C for 5 min, followed by 30 cycles of 94°C for 30 sec, 60°C for 1 min, and 72°C for 2 min, and then a final extension at 72°C for 7 min for LA-Taq, and 30 cycles of 98°C for 5 sec, 55°C for 5 sec, and 72°C for 190 sec for Z-Taq. Next, each region was separately amplified in the 2nd PCR using the 1st PCR product as the template. We used LA-Taq with GC buffer I or II (0.05 U/μl) for amplifying regions from the 5′-flanking region to exon 3 and Ex-Taq (0.02 U/μl, Takara Bio. Inc.) from exons 4 to 6 as described in **Table 1**. The 2nd PCR conditions were 94°C for 5 min, followed by 30 cycles of 94°C for 30 sec, 60°C for 1 min, and 72°C for 2 min, and then a final extension at 72°C for 7 min for all regions. The PCR products were then treated with a PCR Product Pre-Sequencing Kit (USB Co., Cleveland, OH, USA) and directly sequenced on both strands using an ABI BigDye Terminator Cycle Sequencing Kit ver. 3.1 (Applied Biosystems, Foster City, CA, USA) and the sequencing primers listed in **Table 1** (Sequencing). Excess dye was removed by a DyeEx96 kit (Qiagen, Hilden, Germany) and the eluates were applied to an ABI Prism 3730xl DNA Analyzer (Applied Biosystems). All relatively low frequent variations ($n \leq 5$) were confirmed by repeated sequencing analyses of PCR products generated from original (not amplified) genomic DNA. The nucleotide positions based on the cDNA sequence were numbered from the adenine of the translational initiation site or the nearest exons.

Hardy-Weinberg equilibrium and linkage disequilibrium (LD) analyses: Hardy-Weinberg equilibrium and LD analyses were performed by SNPAlyze software ver. 7 (Dynacom Co., Yokohama, Japan). Hardy-Weinberg equilibrium was assessed by the $\chi 2$ test and pairwise LDs between variations were obtained for the frequently used coefficients $|D'|$ and rho square (r^2). $|D'|$ is used to assess the probability for past recombinations, and r^2 is used as a parameter for the linkage between a pair of variations.

Table 1. Primers used for sequencing *FCGRT*

	Enzyme*	Amplified or sequenced region	Forward primer (5′ to 3′)	Reverse primer (5′ to 3′)	Amplified length (bp)
1st PCR	LA-GI	5′-flanking to Exon 3	CTCAGGCTGGTCCTTGAACTCA	ATTAGCCAGTTATGGTGGTATG	5,244
	Z	Exons 4 to 6	CAAGTGTGGTGGTGGGCACCTA	GGGAGTTCGAGACCAGCCTGAT	3,788
2nd PCR	LA-GI	5′-flanking	CTGAACCAGCTGAACGTCCACT	CTGAGCGTGGTGGTGGGCCTGT	1,058
	LA-GII		ATAGAGGTGACAGTTGCACAGC	GGTCCAGACTGACAACAATGCC	1,477
	LA-GII	Exon 1	GAGCAGCAGCCTCCCACAGGAT	ACACAAGAGGCGACAGGTGGTT	1,017
	LA-GI	Exons 2 to 3	ATTGTTGTCAGTCTGGACCG	GCTGCAGTGGGAGGCTGATGGA	1,332
	Ex	Exons 4 to 5	CCAAGGAGGTGACATCTTGAGG	CATCTCTGGGTTTCTGTCTCCA	1,383
	Ex	Exon 6	CCGCCTTGCCGCTGCTGATCCA	GAGCTGAGATCACGCAATTGTA	1,632
Sequencing		5′-flanking	CTGAACCAGCTGAACGTCCACT	CAGGGTCTGGCTCTGTCACTCA	
			GTGCAGAATAGGCAAATCTATC	AACCACATCCTTCTGCTAGGAC	
			CGGGTTCAAGCAATTCTCCTGT	TTGAGGGTGTCTGCCGCTCAGG	
			GAGCAGCAGCCTCCCACAGGAT	CCTCCTCTCTCAGACCCAGGAA	
			CCTGGGTCTGAGGGAGGAGT	CCTCCTCGTACCTGAAGAACTT	
		Exon 1	GGACTCTCAGCCTATCAAGT	ACACAAGAGGCGACAGGTGGTT	
			CCGCGGTGTCCCGGGAGGAA		
		Exons 2 to 3	GTATCTGTCCCACTGCAGTCTA	AACTGAGGCAGGTGGGCATGAC	
		Exon 4	TGAGTCTCTGTCACCTAGGAAG	AGTTAACAGCTCTTCAGACTCA	
		Exon 5	CCGCCTTGCCGCTGCTGATCCA	GTCTCTGTCCTCCCAGGTCTGT	
		Exon 6	TCAGAGAGAGGTGGAGACAGAA	GATGTATAAAACTGGCAGGTTC	
			CCTTGGATCTCCCTTCGTGGAG	TGGCTCACACTTGTAATCCCAC	
			GACGGAGTCTTGCTCTGTTGCT		

*LA-GI: LA-Taq with GC buffer I, LA-GII: LA-Taq with GC buffer II, Z: Z-Taq, Ex: Ex-Taq.

Construction of FcRn expression plasmid: Wild-type human FcRn cDNA was originally obtained from pME18SFL3 (AK075532) (Toyobo, Osaka, Japan). The coding region of FcRn cDNA subcloned into pcDNA3 was amplified by PCR, and then inserted into the EcoRI/SalI site of pEGFP-(C) plasmid. The resulting plasmid encodes hFcRn with C-terminally fused enhanced green fluorescent protein (EGFP) containing the eight amino acid-linker peptide VDSRGSRV between the two proteins. Mutations were introduced by an inverse PCR method. Primers consisted of 5′-AAG GCC CAA CCC AGC AGC CCT GGC TTT-3′ (forward) and 5′-CAG GCG CAT GGA GGG GGG CC CTT CCA-3′ (reverse) for R210Q, 5′-TCC ACC GTC CTC GTG GTG GGA ATC GTC-3′ (forward) and 5′-CTT GGC TGG AGA TTC CAG CTC CAC CCT-3′ (reverse) for S297T. The underlines indicate the mutated nucleotides. The variant plasmids were sequenced on both strands for the entire cDNA region to confirm the introduction of the mutation only at the target sites. Human β2 microglobulin (β2m) cDNA was obtained from pME18SFL3 (FCC106E07) (Toyobo). β2m cDNA was subcloned into pcDNA3.1/
Hygro. The β2m construct was used because FcRn becomes a heterodimer with β2m, which is necessary for the proper intracellular localization of FcRn.[4,5]

Cell culture and plasmid transfection: HeLa cells were cultured in DMEM (Sigma-Aldrich, St. Louis, MO, USA) supplemented with 10% fetal calf serum (Nichirei, Tokyo, Japan). The plasmids encoding the wild-type or variant FcRn fused with EGFP along with the plasmid encoding β2m were transfected into HeLa cells using Lipofectamine 2000 reagent (Invitrogen, Carlsbad, CA, USA) according to the manufacturer's protocol. Plasmids encoding wild-type or variant FcRn fused with EGFP were used for all experiments, including the intracellular localization and antibody recycling activity of FcRn.

Western blot analysis: Wild-type and variant FcRn-EGFP transfected into HeLa cells in 35-mm-diameter dishes were lysed with 500 μL of RIPA buffer [50 mM Tris HCl (pH 7.6), 150 mM NaCl, 1% Nonidet P-40 and 0.25% sodium deoxycholate] supplemented with protease inhibitors (Nacalai Tesque, Kyoto, Japan). After incubation on ice for 30 min, the lysates were centrifuged at 15,000 rpm at 4°C for 20 min. An aliquot (3 μL) of the supernatant was diluted in SDS-sample buffer and applied to 10% SDS-polyacrylamide gel. After electrophoresis, separated proteins were transferred onto polyvinylidene fluoride membrane. Immunochemical detection of FcRn-EGFP proteins was performed using rabbit anti-human FcRn antibody raised against a peptide antigen (residues 135–148, LNGEEFMNFDLKQG). Visualization of the proteins was achieved with horseradish peroxidase-conjugated anti-rabbit IgG antibody (Cell Signaling Technology, Danvers, MA, USA) and the ECL Plus Western blotting detection reagent (GE Healthcare Bio-Sciences AB, Uppsala, Sweden). Protein band densities measured by LAS-3000 (Fuji Film, Kanagawa, Japan) were quantified with Multi Gauge software (Fuji Film).

The relative expression levels are shown as means ± SD of three separate transfection experiments. To verify that the samples were evenly loaded, the blot was reprobed with anti-glyceraldehyde-3-phosphate dehydrogenase (G3PDH) antibody (R&D Systems, Minneapolis, MN, USA).

Fluorescent labeling of antibodies: As a model antibody, we used infliximab, a clinically used chimeric anti-human TNFα antibody which has the Fc domain of human IgG1. The binding of infliximab to human FcRn was shown by surface plasmon resonance analysis in our previous study.[3] Infliximab, kindly provided by Tanabe Pharmaceutical Co. Ltd. (Osaka Japan), was labeled with CypHer5 (GE Healthcare Bio-Sciences, Uppsala, Sweden) by incubating with CypHer5E mono NHS ester in PBS containing 0.5 M Na_2CO_3 (pH 8.3) for 1 hr at room temperature. After the reaction, unbound dye was removed by dialysis in PBS. The protein concentration and degree of labeling were determined by spectrophotometry. IgY (Jackson Immuno Research Laboratories, West Grove, PA, USA) was also labeled with CypHer5 and used in control experiments.

Imaging with fluorescence microscopy: HeLa cells transfected with wild-type or variant FcRn-EGFP cDNA and the β2m cDNA were cultured on 35-mm poly-L-lysine-coated glass-bottom dishes (0.08–0.12 mm thickness) (Matsunami, Osaka, Japan) for 2–4 days. The intracellular localization analyses of wild-type and variant FcRn-EGFP were carried out by confocal laser scanning fluorescence microscopy using a Carl Zeiss LSM510 system (Carl Zeiss, Jena, Germany). For co-localization experiments, wild-type or variant FcRn-EGFP-transfected HeLa cells were incubated with CypHer5-labeled infliximab diluted in cell culture medium containing 200 mM sodium phosphate buffer (pH 6.0) for 2–3 hr at 37°C. Note that throughout this study, the cell culture media used for incubation with the labeled antibody was acidified (pH 6.0) to obtain enhanced incorporation of antibodies into the cells, as reported previously.[6,7] The fluorescent signal was observed in neutral pH medium after washing the cells twice. The 488- and 633-nm laser lines were used to image FcRn-EGFP and CypHer5 labeled-infliximab, respectively.

Biotin labeling of antibodies: Infliximab and IgY were labeled with biotin using EZ-link sulfo-NHS-biotin (Pierce, Rockford, IL, USA). Antibodies and sulfo-NHS-biotin were mixed at the molar ratio of 1:20 and incubated for 60 min at room temperature. Biotinylated antibodies were purified using Zeba desalt spin column (Pierce). Protein concentration was determined by BCA protein assay (Pierce) using bovine serum albumin as a standard.

Recycling assay: HeLa cells were transfected with the wild-type or variant FcRn-EGFP construct along with the β2m construct. The day after transfection, cells were seeded on 96-well plates at 4×10^4 cells/well. After further culturing for one day, recycling assays were performed. Hanks' balanced salt solutions (HBSS) (pH 6.0 and 7.4) were prepared supplemented with 10 mM MES (pH 6.0) and 10 mM Hepes (pH 7.4). The cells were washed with HBSS (pH 7.4) and pre-incubated with HBSS (pH 7.4) for 30 min at 37°C. After washing with HBSS, 10 μg/ml of biotinylated infliximab diluted in HBSS (pH 6.0) containing 0.5% fish gelatin was added to each well. The cells were incubated at 37°C for 1 hr to allow the antibody to be incorporated into the cells. Cells were then washed five times with HBSS (pH 7.4). Then, HBSS (pH 7.4) supplemented with 2% ultra-low IgG FCS (Invitrogen) was added to each well and incubated at 37°C for the indicated periods of time. The supernatant was collected and subjected to ELISA for quantitating the recycled antibody. In order to determine the amount of biotinylated infliximab incorporated into the cells during the 1-hr incubation at 37°C, cells were lysed using RIPA buffer supplemented with protease inhibitors (Nacalai Tesque, Kyoto, Japan) after washing five times with HBSS, and the lysate was subjected to ELISA. Biotinylated IgY was also used as a negative control in some experiments.

Enzyme linked immunosorbent assay (ELISA) for biotinylated antibody: NeutrAvidin (Pierce, Rockford, IL) was bound on Maxisorp 96-well black plates (Thermo Fisher Scientific, Roskilde, Denmark) using IMMUNO-TEK ELISA construction system (ZeptoMetrix, Buffalo, NY, USA). Supernatants or lysates obtained from the recycling assay were applied on the wells and incubated for 16 hr at 4°C. The plates were washed three times with Tris-buffered saline (pH 7.6) containing 0.1% Tween-20 (TBST). Peroxidase-conjugated goat anti-human IgG (Pierce) diluted with TBST was added to the plate and incubated for 1 hr at room temperature. After washing three times with TBST, chemiluminescent reagent (SuperSignal ELISA Femto, Pierce) was added and incubated for 1 min at room temperature. The chemiluminescent signal was detected using an ARVO 1420 multilabel counter (Perkin Elmer, Waltham MA, USA). When the amount of biotinylated IgY was measured, peroxidase-conjugated rabbit anti-chicken IgY (Promega, Madison, WI, USA) was used. For generation of a standard curve, 0.1 to 10 ng/ml of biotinylated corresponding protein was used.

Results

***FCGRT* variations found in a Japanese population:** Thirty-three genetic variations were found, including 17 novel ones, in 126 Japanese subjects (**Table 2**). Of these variations, 14 were located in the 5′-flanking region, 4 (2 synonymous and 2 non-synonymous) in the coding exons, 13 in the introns, 1 in the 3′-untranslated region (UTR), and 1 in the 3′-flanking region. All detected variations were in Hardy-Weinberg equilibrium

Table 2. Summary of *FCGRT* variations detected in this study

SNP ID		Location	Position		Nucleotide change	Amino acid change or known VNTR	Frequency	
This Study	dbSNP (NCBI) or reference		NW_927240.1	From the translational initiation site or from the end of the nearest exon				95% Confidence interval
MPJ6_FRT001[a]		5′-flanking	1557122	−2230	agaacctgaactA > Ccctgaccagcag		0.004	0.000–0.012
MPJ6_FRT002[a]			1557195	−2157	gggtgtcttgcaC > Actgtcatcccag		0.008	0.000–0.019
MPJ6_FRT003	rs78889190		1557207	−2145	cctgtcatcccaG > Ctgctttgggagg		0.020	0.003–0.037
MPJ6_FRT004[a]			1557221	−2131	gctttgggaggcC > Taaggtgggaggc		0.004	0.000–0.012
MPJ6_FRT005[a]			1557498_1557505	−1854_−1847	ggaaggaaggaaGGAAGGAA/-ggaggcaaggaa		0.024	0.005–0.043
MPJ6_FRT006	rs60964075		1557502_1557505	−1850_−1847	ggaaggaaggaaGGAA/-ggaggcaaggaa		0.103	0.066–0.141
MPJ6_FRT007	rs60964075		1557505_1557506	−1847_−1846	ggaaggaaggaaggaa-/GGAAggaggcaaggaa		0.099	0.062–0.136
MPJ6_FRT008[a]			1557505_1557506	−1847_−1846	ggaaggaaggaaggaa-/GGAAGGAAggaggcaaggaa		0.020	0.003–0.037
MPJ6_FRT009[a]			1557506	−1846	ggaaggaaggaaG > Agaggcaaggaag		0.004	0.000–0.012
MPJ6_FRT010[a]			1557540_1557547	−1812_−1805	aaggaaggaaggAAGGAAGG/-aggcaaggaagg		0.004	0.000–0.012
MPJ6_FRT011	rs2335534		1557671	−1681	tctgggagcagcG > Agctgtttaacgg		0.028	0.007–0.048
MPJ6_FRT012[a]			1558366	−986	gatacagaggggT > Gaggaggaggatc		0.004	0.000–0.012
MPJ6_FRT013	ref. 8		1558963_1558999	−389_−353	cgagggtagagcGGTTGGGGGCCCGGACTCCTGG GTCCGAGGGTAGAGC/-ggttgggggccc	VNTR3 > VNTR2	0.032	0.010–0.053
MPJ6_FRT014[a]			1559173	−179	actgagatccagT > Gtcaggggtgaaa		0.028	0.007–0.048
MPJ6_FRT015	rs59774409	Intron 1	1559442	IVS1 + 18	ggccgctccgggC > Tcagggccctgct		0.028	0.007–0.048
MPJ6_FRT016[a]			1559453	IVS1 + 29	gccagggccctgC > Ttgcaggcgggcg		0.147	0.103–0.191
MPJ6_FRT017	rs11551281	Exon 2	1559885	126[b]	ctcgcctgccccG > Tgggactcctgcc	Pro42Pro	0.044	0.018–0.069
MPJ6_FRT018	rs2878342	Exon 3	1560418	582[b]	ggagaggggccgC > Tggaaacctggag	Arg194Arg	0.028	0.007–0.048
MPJ6_FRT019[a]		Exon 4	1570485	629[b]	gcctgaaggcccG > Aacccagcagccc	Arg210Gln	0.004	0.000–0.012
MPJ6_FRT020	rs3810194	Intron 4	1570734	IVS4 + 7	agctgggtgaggT > Ccccgccaggtgg		0.048	0.021–0.074
MPJ6_FRT021	rs1132990		1570857	IVS4 + 130	gccttgaacctcA > Gcgcctgtcagtg		0.048	0.021–0.074
MPJ6_FRT022[a]			1570915	IVS4 + 188	ccaactgccttcC > Tgtctcctgctgc		0.020	0.003–0.037
MPJ6_FRT023	rs10525267		1571020_1571025	IVS4 + 293_ + 298	tgctgctgctgcTGCTGC/-gggtcttcctgg		0.083	0.049–0.117
MPJ6_FRT024[a]			1571170	IVS4–238	ctggcacagcccC > Tgccttgccgctg		0.020	0.003–0.037
MPJ6_FRT025	rs73582442		1571235	IVS4–173	gctggttcttacG > Atccaacctgggg		0.048	0.021–0.074
MPJ6_FRT026	rs73582446		1571314	IVS4–94	gctggaatctccG > Aaggctgggaggg		0.048	0.021–0.074
MPJ6_FRT027[a]		Exon 5	1571425	889[b]	ccagccaagtccT > Accgtgctcgtgg	Ser297Thr	0.020	0.003–0.037
MPJ6_FRT028	rs55662447	Intron 5	1571614_1571615	IVS5 + 90_ + 91	agagacccagagAG/-gggggacagaga		0.028	0.007–0.048
MPJ6_FRT029[a]			1571615	IVS5 + 91	gagacccagagaG > Tgggggacagaga		0.004	0.000–0.012
MPJ6_FRT030	rs77741672		1571691	IVS5 + 167	gagaggggggacgG > Cagacagagaccc		0.151	0.107–0.195
MPJ6_FRT031[a]			1571915	IVS5–46	gtcagacccagaG > Acgcctcagagat		0.020	0.003–0.037
MPJ6_FRT032	rs14769	3′-UTR	1572276	1304 (*206)[c]	taacacgagtttG > Aggcccgaatcag		0.044	0.018–0.069
MPJ6_FRT033[a]		3′-flanking	1572364	1312 + 80 (*214 + 80)[d]	tgggcctcggatC > Ttctcctacaggt		0.004	0.000–0.012

[a]Novel variations detected in this study.
[b]Positions in cDNA (NM_004107.3).
[c]Numbered from the termination codon TGA.
[d]Positions were shown as 1312 (*214) (final base of exon 6) + bases from the end of exon 6.